

Research Article

A Time-Domain Fingerprint for BOC(m, n) Signals

B. Muth,¹ P. Oonincx,¹ and C. Tiberius²

¹ Faculty of Military Sciences, Netherlands Defence Academy, Het Nieuwe Diep 8, 1781 AC Den Helder, The Netherlands

² Department of Earth Observation and Space Systems (DEOS), Delft University of Technology, Kluyverweg 1, 2629 HS Delft, The Netherlands

Received 3 November 2006; Accepted 10 April 2007

Recommended by Sudharman Jayaweera

Binary offset carrier (BOC) describes a class of spread-spectrum modulations recently introduced for the next generation of global navigation satellite systems (GNSSs). The design strategies of these BOC signals have so far focused on the spectral properties of these signals. In this paper, we present a time-domain fingerprint for each BOC signal given by a unique histogram of counted time elapses between phase jumps in the signal. This feature can be used for classification and identification of BOC-modulated signals with unknown parameters.

Copyright © 2007 B. Muth et al. This is an open access article distributed under the Creative Commons Attribution License, which permits unrestricted use, distribution, and reproduction in any medium, provided the original work is properly cited.

1. INTRODUCTION

In the scope of emerging radionavigation satellite systems, the binary offset carrier (BOC) modulation is of special interest. The new generation of global navigation satellite systems (GNSSs), modernized GPS [1], and the European Galileo system [2] will use BOC (or BOC-based) signals on different carriers and with different parameters, to enable ranging. The main reasons for creating BOC signals were, on one hand, the need to improve traditional GNSSs signals properties for better resistance to multipath interferences of all kinds and receiver noise [3, 4], and on the other hand, the need for improved spectral sharing of the allocated bandwidth with existing signals or future signals of the same class [3, 5]. Particularly, correlation and spectral properties were improved during the BOC design process. The improvements for the acquisition and tracking of future GNSSs signals have been assessed and new algorithms have been elaborated. We study the behaviour of BOC signals from a different point of view, namely, by counting and accumulating time elapses between phase jumps in the signal.

The paper is organised as follows. After introducing BOC(m, n) signals in Section 2, we study the statistical behaviour of the length of time intervals between phase jumps in BOC(m, n) signals in Sections 3 and 4. We refer to these time intervals as run lengths and will not focus on their computation. Studying these run lengths will be based upon arithmetic relationships between the BOC parameters m

and n , using some elementary combinatorial relations. In Section 5, convergence results for the obtained statistics are derived as a function of the number of measured code chips. Furthermore, we present examples of distributions of run lengths derived for specific parameters m and n to illustrate the results. Finally, some conclusions and directions for further research are presented in Section 6. In this perspective, we also briefly discuss related signal structures, like MBOC and cosine-phased BOC.

2. BINARY OFFSET CARRIER SIGNAL

A BOC-modulated signal consists of a sinusoidal carrier, a subcarrier, a pseudorandom noise (PRN) spreading code, and a data sequence. The BOC signal is the product in the time domain of these components. To investigate the appearances of singularities (jumps) in a BOC signal we focus on the product of the subcarrier waveform and the spreading code sequence. Since the sinusoidal carrier is continuous and thus does not contribute to any phase jump in the modulated signal, we do not take the behaviour of this carrier wave into account in the sequel of this paper. Furthermore, the data sequence is not taken into account, since it usually has a far lower frequency than all other components [6].

To introduce BOC signals, we take $2T_s$ (resp., f_s) as the subcarrier period (resp., frequency). For the subcarrier several waveforms are possible. In this paper, we will limit our study to the case of a rectangular sine-phased subcarrier. Besides, we will refer to the spreading symbols (resp., sequence)

in the code as pseudo-random noise (PRN) chips (resp., code). The length (resp. chipping rate or code rate) of such a PRN chip is denoted by T_c (resp., f_c). Physically, that means that the code might change (but not necessarily) from -1 to $+1$ and conversely every $1/f_c$ second. In addition, we assume that the spreading code is a sequence of independent and identically distributed random variables. As a result, we do not take into account any additional requirements on the correlation function of the spreading code, for example, see [7]. The reason for doing this is that in our study we only consider a limited number of code chips, while the mathematical requirements on the code can only be verified when considering the whole code, containing much more code chips.

GNSSs satellites have an atomic clock on-board with a nominal reference frequency f_0 from which all components of the generated navigation signals are derived. In case of a BOC signal, besides the carrier frequency also the subcarrier frequency f_s and the code rate f_c are multiples of f_0 , that is, $f_s = m \cdot f_0$, $f_c = n \cdot f_0$. The BOC signal with subcarrier frequency $m f_0$ and code rate $n f_0$ is referred to as BOC(m, n). For the sake of simplicity, m and n are assumed to be positive integers, with $m \geq n$, which is the case in practice. Signals like BOC(15, 2.5) also appear in literature. Such type of signals is intended for specific services such as the galileo public regulated service (PRS) to be of interest for experts. As we will see in the next section only the division of m by n is of importance for the results in this paper, not the values of m and n themselves.

Although in this paper we will only concentrate on the code subcarrier product within a BOC signal, here we briefly mention the formal time and frequency representation of a BOC signal. The complex envelope representation of the BOC signal is given by

$$s(t) = \exp(-i\theta) \sum_j a_j \cdot \mu_{kT_s}(t - jkT_s - t_0) \cdot c_{T_s}(t - t_0), \quad (1)$$

with a_j the sequence of data-modulated spreading code values, $\mu_{kT_s}(t)$ the spreading symbol of duration $T_c = kT_s$, $c_{T_s}(t)$ the subcarrier of period $2T_s$ and k the number of subcarrier half-periods during which the spreading code value remains unchanged. The frequency spectrum of a BOC(f_s, f_c) signal reads for k , even,

$$G(f) = \frac{1}{kT_s} \left(\frac{\sin(\pi f T_s) \sin(k\pi f T_s)}{\pi f \cos(k\pi f T_s)} \right)^2 = f_c \left(\frac{\tan(\pi f / 2 f_s) \sin(\pi f / f_c)}{\pi f} \right)^2. \quad (2)$$

Whereas for k odd, we have

$$G(f) = \frac{1}{kT_s} \left(\frac{\sin(\pi f T_s) \cos(k\pi f T_s)}{\pi f \cos(k\pi f T_s)} \right)^2 = f_c \left(\frac{\tan(\pi f / 2 f_s) \cos(\pi f / f_c)}{\pi f} \right)^2. \quad (3)$$

For the derivation of the BOC spectrum we refer to [3].

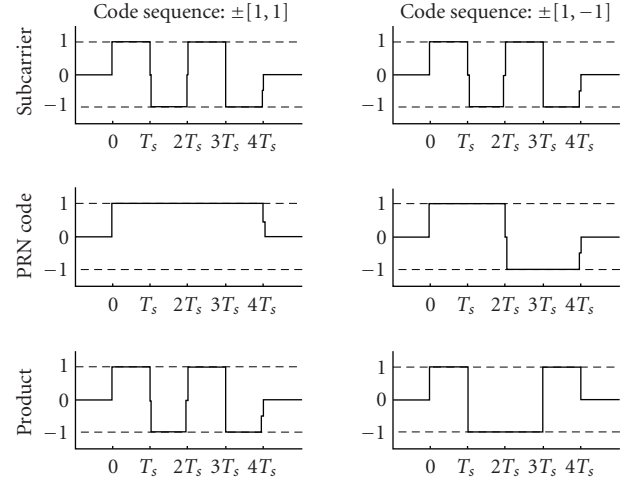


FIGURE 1: Product of BOC(1, 1) subcarrier and spreading code for two code possibilities.

3. RUN LENGTH HISTOGRAMS FOR BOC($kn/2, n$)

The time-domain fingerprint for BOC signals we introduce in this paper is based on the time elapses between consecutive phase jumps in a BOC signal. These phase jumps are due to jumps (discontinuities) in the code subcarrier product. In Figure 1, five of such jumps are shown in the left-hand example and four of such transitions show up in the right-hand example. The time elapses between these jumps (T_s at the left and T_s and $2T_s$ at the right) are referred to as run lengths.

As a starting point for studying run length appearing in BOC(m, n) signals is to consider the class BOC($m, 1$), $m = 1, 2, 3, \dots$. Results for BOC($kn/2, n$), with integer k , are obtained straightforwardly from this BOC($m, 1$) case. Moreover, an extension of the method used for deducing the BOC($m, 1$) results will be used in the next section for yielding results on the run lengths for general BOC(m, n) signals, with $m \geq n$.

We will first concentrate on BOC($m, 1$) as a special case of BOC($kn/2, n$) with $k = 2m, n = 1$. For BOC($m, 1$) signals, we consider sections of length pT_c containing exactly p PRN chips. Since $T_c = mT_s$, pm half periods of the subcarrier may appear during such a section. Here a half period is considered as an interval of half the length of the subcarrier's period, that is also marked by a parity jump in the code subcarrier product. We identify one half period with its length T_s .

The number of half periods appearing in the combined BOC signal during p PRN chips also depends on the spreading code. If a code is changing state, then the product of code and subcarrier will not change its state at that particular moment in time, yielding an extension of that spreading-code half period to a full period. Then the number of half periods T_s , indicated by $N(T_s)$, is divided by a factor 2 and the number of full periods $2T_s$, given by $N(2T_s)$, increases by 1. We observe, that for BOC($m, 1$), only full and half periods can appear like this, since the state jumps of the chips always coincide with jumps of the subcarrier.

TABLE 1: BOC($m, 1$) run length counts for all possible code subcarrier combinations.

Number of PRN chips p	Number of half periods T_s	Number of periods $2T_s$	Number of code possibilities	Code possibilities
2	$4m (2 \cdot 2m)$	0	1	[1, 1]
	$4m - 2 (2 \cdot 2m - 2)$	1	1	[1, -1]
3	$6m (3 \cdot 2m)$	0	1	[1, 1, 1]
	$6m - 2 (3 \cdot 2m - 2)$	1	2	[1, 1, -1] [-1, 1, 1]
	$6m - 4 (3 \cdot 2m - 4)$	2	1	[1, -1, 1]
	$8m (4 \cdot 2m)$	0	1	[1, 1, 1, 1] [-1, 1, 1, 1]
4	$8m - 2 (4 \cdot 2m - 2)$	1	3	[1, 1, -1, -1] [1, 1, 1, -1] [-1, 1, 1, 1]
	$8m - 4 (4 \cdot 2m - 4)$	2	3	[-1, 1, 1, 1] [-1, 1, 1, 1]
	$8m - 6 (4 \cdot 2m - 6)$	3	1	[1, -1, 1, -1]

To illustrate these considerations we take as an example BOC(1,1) during $p = 2$ PRN chips as depicted in Figure 1. Two possible situations can appear. First, in case the PRN sequence is $\pm[1, 1]$, the product of code and subcarrier contains 4 run lengths of duration T_s (left graph). Second, in case the PRN sequence is $\pm[1, -1]$, the second and third half periods have the same state and are therefore merged to one full periods time interval. So, in this case, the product of code and subcarrier contains 2 run lengths of duration T_s and 1 of duration $2T_s$ (right graph).

We can follow the same observations for BOC($m, 1$) signals for $p = 2, 3, 4$. The appearances of half and full periods (T_s versus $2T_s$) between parity changes in the code subcarrier product have been counted for all possible combinations of code and subcarrier. The results can be found in Table 1. There the second and third columns show the number of half and full periods that can appear in one code subcarrier product within a duration of p code chips. In the fourth column, the number of different code combinations that can appear in the various situations is indicated.

What can be observed from Table 1 is that, for $N(T_s)$, multiples of 2 are subtracted from $2pm$, each time $N(2T_s)$ is increased by 1. Also we note that the number of possible codes follows binomial coefficients. In fact, these numbers should be multiplied by 2, since all codes also have a counterpart (multiply code by -1). However, for our computations, we identify the counterparts with the original codes.

Extrapolating the observations of Table 1 for higher values of p , we derive expressions for the expected values of $N(T_s)$ and $N(2T_s)$. This is done by accumulating all 2^{p-1} possible combinations and taking the mean, that is,

$$\begin{aligned}
 N(T_s) &= 2^{1-p} \sum_{k=0}^{p-1} \binom{p-1}{k} (2pm - 2k), \\
 N(2T_s) &= 2^{1-p} \sum_{k=0}^{p-1} \binom{p-1}{k} k.
 \end{aligned} \tag{4}$$

Using a corollary of Newton's binomial theorem, (4) can be rewritten as

$$N(T_s) = 2^{1-p} (2pm \cdot 2^{p-1} - 2(p-1) \cdot 2^{p-2}) = 2pm - p + 1, \tag{5}$$

$$N(2T_s) = 2^{1-p} \cdot (p-1)2^{p-2} = \frac{p-1}{2}. \tag{6}$$

For large p , a distribution of the two types of run lengths in BOC($m, 1$) is obtained by taking

$$\lim_{p \rightarrow \infty} \frac{N(T_s)}{N(2T_s)} = \lim_{p \rightarrow \infty} \frac{4pm - 2p + 2}{p - 1} = 4m - 2. \tag{7}$$

This means that for reasonable large p a fraction of $1/(4m-1)$ of all intervals between phase jumps in BOC($m, 1$) is of length $2T_s$, and $(4m-2)/(4m-1)$ of those intervals are of length T_s . Typically for BOC(1,1) we have an expected distribution of 1/3 versus 2/3.

An extension of the previous results yields the distribution of run lengths for signals of type BOC($kn/2, n$), since for these signals the characteristics and construction of the code subcarrier product coincide with those of BOC($k, 2$) up to a division/multiplication of T_c and T_s by n . As a result for BOC($kn/2, n$), we have the same run length statistics as for BOC($k/2, 1$). More general, in the case of BOC(m, n) with n a divisor of $2m$, the distribution of length $2T_s$ intervals versus length T_s intervals in the signal is given by $1/(4m/n-1) = n/(4m-n)$ versus $(4m/n-2)/(4m/n-1) = (4m-2n)/(4m-n)$. As a special case we have the distribution 1/3 versus 2/3 for all BOC(m, m).

4. RUN LENGTH RESULTS FOR ARBITRARY BOC(m, n)

One may easily verify that all types of BOC(m, n) signals discussed in the previous section satisfy $\gcd(2m, n) = n$ (greatest common divisor). Here we discuss all other possibilities, namely, $1 \leq \gcd(2m, n) < n$, starting with $\gcd(2m, n) = 1$,

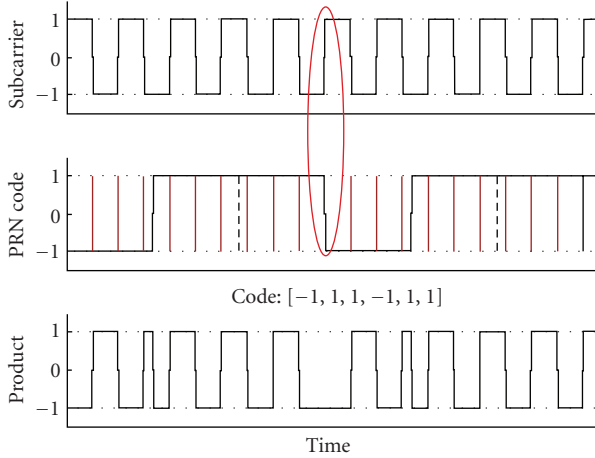


FIGURE 2: Components of a BOC(5,3) signal in the time-domain. The vertical solid indicators displayed over the code correspond to the subcarrier phase jumps, whereas the dashed indicators in the PRN code correspond to the possible transitions in the code state. The ellipse illustrates the first observation made in this section, namely, the coincidence of the n th possible code change with the $2m$ th subcarrier state change.

that is, $2m$ and n are relatively prime. Translated in terms of the code subcarrier product we observe that

- (i) Every n th possible code change coincides with every $2m$ th phase jump in the subcarrier;
- (ii) Between such coinciding phase jumps, $n - 1$ possible code changes do not coincide with subcarrier jumps, but intersect $2m$ subcarrier half periods.

These observations have been depicted for BOC(5,3) in Figure 2.

The run length statistics can be obtained by construction, with respect to these two observations. Considering only the first observation, we would have the same run length statistics as for BOC($m, 1$). The second observation introduces the possibility of having $n - 1$ other run length values $(i/n)T_s$, $i = 1, 2, \dots, n - 1$ by intersection, that all may appear twice within n chips. This double counting is due to the fact that a code change first yields a run length contribution of $(i/n)T_s$ and $((n - i)/n)T_s$, and at a later stage may contribute with lengths of $((n - i)/n)T_s$ and $(i/n)T_s$. The construction of this BOC(m, n) run length distribution with $\gcd(2m, n) = 1$ is also illustrated in Figure 4. We start from the steady distribution for BOC($m, 1$), given by $N(T_s) : N(2T_s) = 4m - 2 : 1$ (see Figure 3). Next, $m - 1$ intervals of length T_s may be divided into two smaller intervals of length kT_s/n and $(n - k)T_s/n$. Concluding, for this type of BOC(m, n), we obtain the relation

$$\begin{array}{ccccccc} N(T_s/n) & : & N(2T_s/n) & : & \dots & : & N((n-1)T_s/n) & : & N(T_s) & : & N(2T_s) \\ 2 & : & 2 & : & \dots & : & 2 & : & 4m-2-(n-1) & : & 1 \end{array} \quad (8)$$

or equivalently, for large p , a fraction of $1/(4m + n - 2)$ of all intervals between phase jumps in BOC(m, n) is of length $2T_s$,

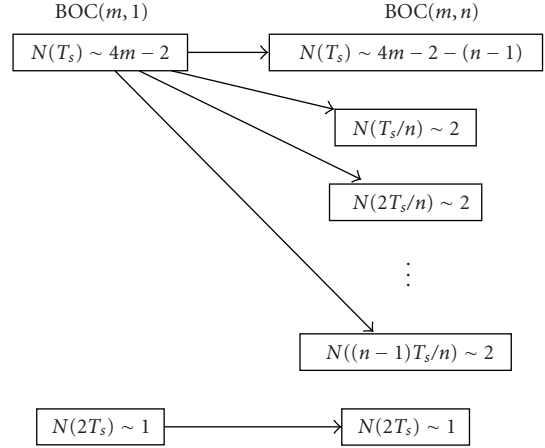


FIGURE 3: Starting with the steady distribution for BOC($m, 1$) (left); the distribution for BOC(m, n) (right) is obtained by splitting T_s run lengths.

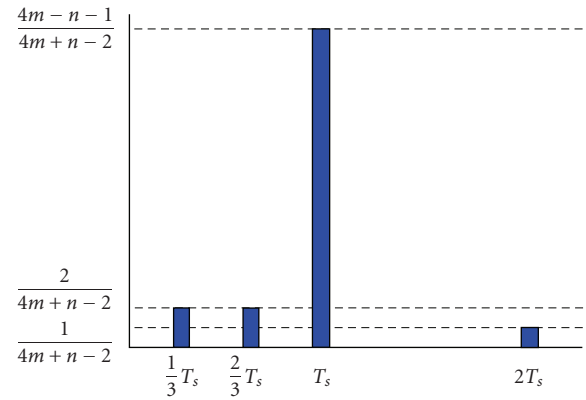


FIGURE 4: Run length histogram of a BOC(5,3) signal.

$(4m - n - 1)/(4m + n - 2)$ of those intervals are of length T_s , and $n - 1$ intervals of length $(i/n)T_s$, $i = 1, \dots, n - 1$, appear with probability $2/(4m + n - 2)$.

Resuming, for large p , the relation $N(T_s) : N(2T_s)$ is taken from the previous section, that is, $4m - 2 : 1$ following the results for BOC($m, 1$). Next, $n - 1$ half periods are divided into intervals separating phase jumps with duration $(1/n)T_s, \dots, ((n - 1)/n)T_s$ all appearing twice in mean.

As an example, we consider again a BOC(5,3) signal. The run length statistics (Figure 4) obtained for this signal show four different intervals of length $T_s/3, 2T_s/3, T_s$, and $2T_s$ with distributions $2/21, 2/21, 16/21$, and $1/21$, respectively.

As in the previous section also the latter results can be extended in a rather straightforward way. In case we are dealing with BOC(m, n) with $1 < \gcd(2m, n) < n$, we may consider BOC($m/c, n/c$), with $c = \gcd(2m, n)$. Since this type of signals only differs from BOC(m, n) by means of a division/multiplication of T_c and T_s by c , the same run length statistics as for BOC(m, n) with $1 < \gcd(2m, n) < n$ apply for BOC($m/c, n/c$). Furthermore, we have $\gcd(2m/c, n/c) = 1$, so that we can use the previously obtained results. Following

these results, we have a portion of $c/(4m+n-2c)$ of all intervals between phase jumps of length $2T_s$, $(4m-n-c)/(4m+n-2c)$ of those intervals of length T_s and $n/c-1$ intervals of length $i(c/n)T_s$, $i=1, \dots, n/c-1$, appear with probability $2c/(4m+n-2c)$.

Reviewing the five different cases that cover all different BOC(m, n), $m \geq n$, we observe that every single case can be regarded as a special case of the latter case in which $1 < \gcd(2m, n) < n$. Therefore, the run length statistics for arbitrary BOC(m, n) read as in Table 2.

5. CONVERGENCE AND EXPERIMENTAL RESULTS FOR RUN LENGTH STATISTICS

In this section, we discuss the results as presented in Table 2 from a practical point of view. First we will derive an approximation result, that yields an indication of the number of chips to be taken into account before the steady distribution of Table 2 is achieved up to a given accuracy. Next, experimental results for different BOC(m, n) will illustrate accuracy and correctness of the statistics in practice.

The derived statistics hold in case many chips (in time) are considered at different positions in the signal. However, the exact number of chips necessary to approximate the steady distribution does not follow from the derivations in the previous section. To give insight in this convergence behaviour we consider BOC($kn/2, n$)-type of signals and derive an expression for the number of code chips to be considered before the distribution from Table 2 is obtained up to a given accuracy.

For $m = kn/2$ we use (6) to get the fraction of $2T_s$ run lengths after p chips, given by

$$\frac{N(2T_s)}{N(T_s) + N(2T_s)} = \frac{(p-1)/2}{2pm/n - p/2 + 1/2} = \frac{np - n}{4pm - np + n}. \quad (9)$$

According to Table 2, we have to compare (9) with $n/(4m-n)$, the fraction's value in limit. The relative error in the statistics for $N(2T_s)$ is now given by

$$\begin{aligned} E_{m,n}(p) &= \left| \frac{n/(4m-n) - ((np-n)/(4pm-pn+n))}{n/(4m-n)} \right| \\ &= \left| 1 - \frac{(4m-n)(p-1)}{4pm-pn+n} \right| \\ &= \left| 1 - \frac{4pm-pn+n-4m}{4pm-pn+n} \right| = \frac{4m}{p(4m-n)+n}. \end{aligned} \quad (10)$$

The number of chips p to be considered for obtaining an accuracy δ in the relative error is calculated from $E_{m,n}(p) \leq \delta$. Rewriting this inequality using (10) yields

$$p > \frac{4m - \delta n}{4\delta m - \delta n}. \quad (11)$$

We observe that for small δ the minimum number of chips p needed for accuracy δ tends to

$$p \approx \frac{4m}{\delta(4m-n)}. \quad (12)$$

TABLE 2: BOC(m, n) run length statistics with $c = \gcd(2m, n)$.

Run length	Fraction in distribution
$i \frac{cT_s}{n}$, $i=1, \dots, n/c-1$	$\frac{2c}{4m+n-2c}$
T_s	$\frac{4m-n-c}{4m+n-2c}$
$2T_s$	$\frac{c}{4m+n-2c}$

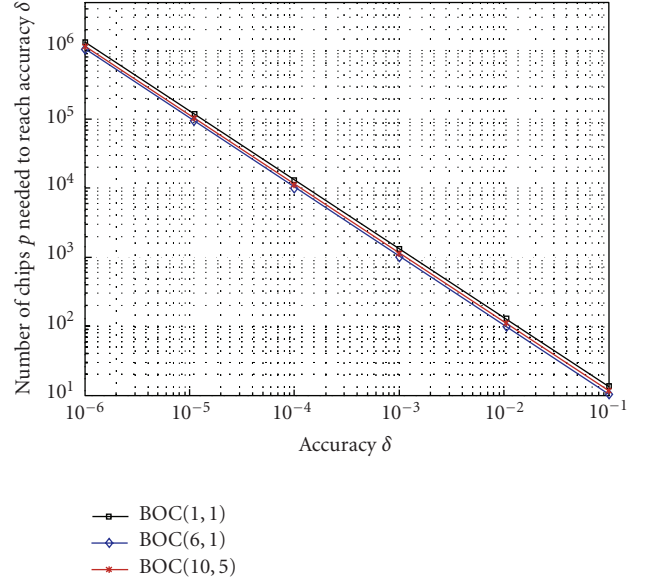


FIGURE 5: Number of chips p needed to reach accuracy δ for different BOC signals.

Figure 5 depicts the logarithmic dependence of the number of chips p to the required accuracy δ for different BOC signals with parameters (1, 1), (6, 1), and (10, 5).

Similar computations also hold for expressing the relative error in the steady results for $N(T_s)$. It can be derived (left to the reader) that for $N(T_s)$ we have a relative error

$$\tilde{E}_{m,n}(p) = \frac{2mn/(2m-n)}{p(4m-n)+n}. \quad (13)$$

We will not elaborate further on this relative error, since the error in $N(2T_s)$ always is the largest and therefore seems to be the best quality measure for the statistics.

We remark that the results obtained here only hold in case the expected values for the distribution after p chips are accurate. This can be achieved by taking a large number of p -chip intervals into account and averaging the distributions.

For several types of BOC(m, n) signals the distributions of run lengths have been calculated during a 7- microsecond simulation. Figure 6 shows the calculated run length distribution for a simulated BOC(10, 5) signal. As can be seen in the figure, already a simulation of 36-code chips yields a result close to the derived steady distribution. Since

this simulation was only done for a small number of 7-microsecond time interval, the values of the steady distribution are not accurate enough, resulting in a relative error $E_{10,5}(p)$ that is larger than the theoretical error.

Figure 7 shows the distribution of runs length for a BOC(7,3) signal. Since this situation corresponds to the case where n does not divide $2m$ more run lengths appear, namely, $T_s/3$, $2T_s/3$, T_s , and $2T_s$. In this experiment, more chips than in Figure 6 have been considered yielding a better approximation.

6. CONCLUSIONS AND FUTURE RESEARCH

In this paper, we introduced an identification of a BOC(m, n) signal through a unique histogram. Indeed, measuring the duration of time intervals between phase jumps and counting them leads to a distribution depending only on the BOC parameters m and n . Although similar histograms may show up for different BOC(m, n), the values of T_s will differ in these cases resulting in unique fingerprints. If n divides $2m$ only subcarrier half periods (T_s) and full periods ($2T_s$) are observed in the BOC(m, n) signal with respective probabilities of occurrence $(4m - 2n)/(4m - n)$ and $n/(4m - n)$. Otherwise, if n and $2m$ are relatively prime, $n + 1$ possible run length exist, namely, subcarrier half-periods (T_s), full periods ($2T_s$) with respective probabilities $(4m - n - 1)/(4m + n - 2)$ and $1/(4m + n - 2)$ and also intervals equal to $(iT_s/n)1, \dots, n - 1$ each appearing with a probability equal to $2/(4m + n - 2)$.

The analysis described in this paper can only be performed in case most phase jumps in the signal can be identified. In case a reasonably large number of chips are considered, not having identified some phase jumps is not a huge problem. This is due to the fact that these mismatches will disappear when matching steady distributions for classifying the signals. In practice, this means that the method also can be applied to noisy signals with reasonable SNR values. Moreover, also the type of BOC(m, n) plays a role in accurate classification in noisy environments. Small run lengths (high values of n) and small jumps in the combined BOC signal may disappear in the noise more easily than other type of phase jumps. A better description of this topic is subject to further research.

Further research is also needed to find out whether, with the same statistical approach, identification of other BOC-based signals is possible. One can think of the recently introduced MBOC class of signals and BOC signals based on different spreading waveforms, see [7]. We expect that our method can be adapted more or less straightforwardly for time-multiplexed BOC (TMBOC) signals, since this is a time-domain arrangement of different BOC signals, as treated in this paper. Since the idea behind our approach is not affected by the position of the phase jumps, we expect the method also to be applicable to cosine-phased BOC. However, more research is needed for finding the exact shape of the run length histograms for variations on BOC signals and for answering the question of uniqueness of such new statistics.

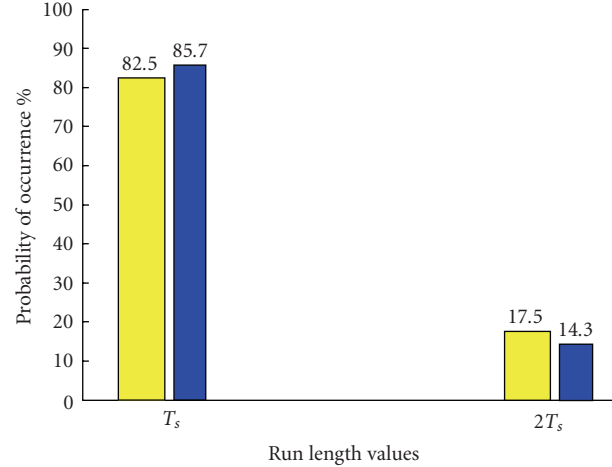


FIGURE 6: Histogram of the run lengths of a BOC(10,5) signal of duration $7 \mu\text{s}$ (corresponding to 36 code chips). The lighter bars account for the computed experimental probabilities, whereas the darker bars make up for the theoretical probabilities.

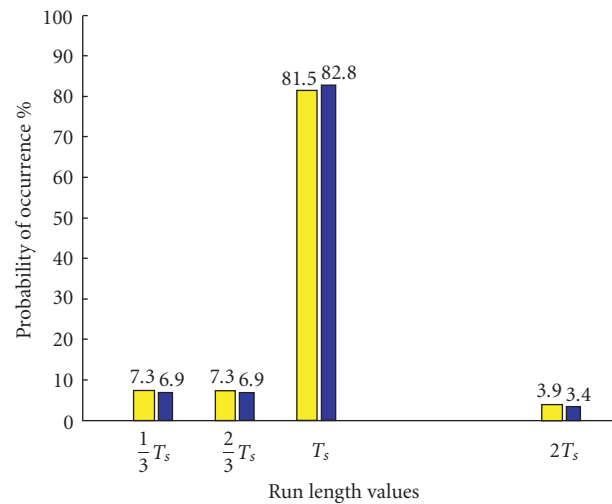


FIGURE 7: Histogram of the run lengths of a BOC(7,3) signal of duration 1 ms (corresponding to 3069 code chips). The lighter bars account for the computed experimental probabilities, whereas the darker bars make up for the theoretical probabilities.

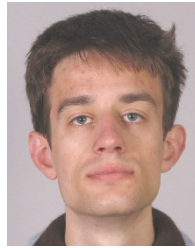
REFERENCES

- [1] J. W. Betz, "The offset carrier modulation for GPS modernization," in *Proceedings of the National Technical Meeting of the Institute of Navigation (ION NTM '99)*, pp. 639–648, San Diego, Calif, USA, January 1999.
- [2] G. W. Hein, J.-A. Avila-Rodriguez, L. Ries, et al., "A candidate for the Galileo L1 OS optimized signal," in *Proceedings of the 18th International Technical Meeting of the Satellite Division of the Institute of Navigation (ION GNSS '05)*, pp. 833–845, Long Beach, Calif, USA, September 2005.
- [3] J. W. Betz, "Binary offset carrier modulations for radionavigation," *Journal of The Institute of Navigation*, vol. 48, no. 4, pp. 227–246, 2001.

- [4] J. K. Holmes, S. Raghavan, P. Dafesh, and S. Lazar, "Effective signal to noise ratio performance comparison of some GPS modernization signals," in *Proceedings of the 12th International Technical Meeting of the Satellite Division of the Institute of Navigation (ION GPS '99)*, pp. 1755–1762, Nashville, Tenn, USA, September 1999.
- [5] J.-A. Avila-Rodriguez, G. W. Hein, S. Wallner, T. Schueler, E. Schueler, and M. Irsigler, "Revised combined Galileo/GPS frequency and signal performance analysis," in *Proceedings of the 18th International Technical Meeting of the Satellite Division of the Institute of Navigation (ION GNSS '05)*, pp. 846–860, Long Beach, Calif, USA, September 2005.
- [6] Galileo Joint Undertaking, "Galileo Open Service Signal in Space Interface Control Document (OS SIS ICD) Draft 0," May 2006.
- [7] G. W. Hein, J.-A. Avila-Rodriguez, S. Wallner, et al., "MBOC: the new optimized spreading modulation recommended for Galileo L1 OS and GPS L1C," in *Proceedings of the IEEE/ION Position, Location, and Navigation Symposium (PLANS '06)*, pp. 883–892, San Diego, Calif, USA, April 2006.

He is involved in international projects on satellite navigation, in particular on the European EGNOS augmentation system and Galileo.

B. Muth graduated in June 2005 from the Electronics Department of the ENSEEIHT engineering school in Toulouse, France. He obtained both the engineering degree and the M.S. degree with specialisation in signal processing. His M.S. thesis research, carried out at the French-German Institute ISL of Saint-Louis, France, focused on environmental noise canceling for acoustic localization of snipers. Since December 2005, he is working as a Ph.D. student in a joint project of The Netherlands Defense Academy and the Mathematical Geodesy and Positioning group at the Aerospace Engineering Faculty, Delft University of Technology, The Netherlands. His research focuses on time-frequency digital signal processing solutions for global navigation satellite systems software receivers.



P. Oonincx received his M.S. degree (with honors) in mathematics from Eindhoven University in 1995 with a thesis on generalizations of multiresolution analysis. In 2000, he received the Ph.D. degree in mathematics from University of Amsterdam. His thesis on the mathematics of joint time-frequency/scale analysis has also appeared as a textbook. Currently, he works as an Associate Professor in mathematics and signal processing at The Netherlands Defense Academy, Den Helder, The Netherlands. His research interests are GNSSs signal processing, wavelet analysis, time-frequency signal representations, multiresolution imaging, and signal processing for geophysics.



C. Tiberius obtained his Ph.D. degree in 1998 at Delft University of Technology on recursive data processing for kinematic GPS surveying. His research interest lies in radio-navigation, primarily with global navigation satellite systems. He is currently an Assistant Professor in the Delft Institute of Earth Observation and Space Systems (DEOS), and responsible for courses on data processing and navigation.

